



Mid-Infrared Astronomy with IRAIT at Dome C: performances and simulations

M. Fiorucci^{1,3}, P. Persi², M. Busso¹, S. Ciprini^{1,3}, L. Corcione⁴, G. Tosti^{1,3}

¹ Dipartimento di Fisica, Università di Perugia, via Pascoli, 06123 Perugia

² Consiglio Nazionale delle Ricerche (CNR), IAS, Torvergata, 00133 Roma

³ INFN, Sezione di Perugia, via Pascoli, 06123 Perugia, Italy

⁴ INAF Osservatorio Astronomico di Torino, 10025 Pino Torinese (TO), Italy

Abstract. In the Antarctic Continent there are sites, such as Dome C, where the ambient conditions are expected to be favourable to open new windows to the Universe in the mid-infrared. Here we present the expected performances and simulated results of the mid-IR array camera for astronomy that we are developing for the IRAIT telescope. The optical configuration will permit a sensitivity of 4 mJy at 10 μm , considering a 10% bandwidth filter, the source in one beam, 1 sigma, and one hour integration time in chop-nod.

Key words. Infrared - Astronomical Instrumentation - Photometry - Antarctica

1. Introduction

The Antarctic Plateau features the best atmospheric conditions on Earth for infrared astronomical observations (see, e.g., Chamberlain et al. 2000). The cold atmosphere, high-altitude, low water-vapor content and the relative stability of the weather provide conditions that are superior to any other ground-based site. Atmospheric windows in the mid-infrared will become accessible, in particular from 17 to 30 μm (see, e.g., Hidas et al. 2000), a spectral region that is scarcely accessible in temperate sites.

The Franco-Italian Concordia Station (Dome C) will be operational in 2004, and some persons could spend winter there. The

qualification of the astronomical site and the first observations in the mid-infrared are therefore scheduled for the first winters. For this purpose, the Italian Robotic Antarctic Infrared Telescope (IRAIT, see Tosti 2003) will be placed at Dome C during 2005.

The IRAIT project is based on a fully robotic 80 cm telescope, with a collecting area $\sim 0.5 \text{ m}^2$, focal ratio f/20 and optical scale of 12.9 arcsecs/mm. With this telescope the Airy disc has a diameter of 6.3 arcsecs at 10 μm , and 12.6 arcsecs at 20 μm . The telescope will be soon equipped with a mid-infrared camera to measure the real capabilities of the site. The camera will be an upgrade of TIRCAM (Persi et al. 1994) and TIRCAM2 (Persi et al. 2002). We have decided to use the same kind of detector because of the good results ob-

Send offprint requests to: M. Fiorucci
Correspondence to: fiorucci@pg.infn.it

Table 1. Requirement and performance of the camera

Array characteristics		System Requirement	
Array Temperature	5-10°K	System Transfer Gain	$\sim 1500 e^-/\text{ADU}$
N. of pixels	128×128	Readout Noise	$< 10^3 e^-$
Pixel size	$75 \times 75 \mu\text{m}^2$	A/D Toggle Noise	$\sim 0.7 \text{ ADU}$
Well Capacity	$2 \times 10^7 e^-$	Field of View	$\sim 4' \times 4'$
Dark Current	$10^6 e^-/\text{s}/\text{pixel}$ (7°K)	Pixel Scale	$\sim 2 \text{ arcsec}/\text{pixel}$
Quantum Yield (ηG)	~ 0.7 (7°K)	Optics	reflective

tained with the previous camera, and to guarantee prompt results soon after the installation. The choice of a high-flux Si:As array will permit to test the extended observational windows in the 20-30 μm spectral region, thanks to the exceptional observational conditions expected at Dome C. Table 1 summarizes the expected characteristics of the camera, estimated taking into account the characteristics of the existing TIRCAM2 (see Corcione et al. 2003). The optical scheme of the camera will produce a demagnification $F \simeq 770\text{cm}$, for a scale in the focal plane of 26.7 arcsec/mm, a scale that satisfies the Nyquist criterion at 8-9 μm and that is anyway acceptable around 20 μm .

2. Estimated performances of the camera

To evaluate the performances of the camera, we need the assumption of many parameters that can be correctly measured only after the real construction and final assembly. However, we can evaluate many of them thanks to a reasonable knowledge of the array, and the site-testing done in Antarctica.

Figure 1 shows the assumed mean atmospheric transmission at Dome C, derived from the considerations of Chamberlain et al. (2000), and Hidas et al. (2000).

The telescope and camera transmission is assumed as 0.80 at all the working wavelengths.

The background brightness is strongly affected by the emissivity of the telescope,

since the expected sky emission at the high Antarctic Plateau is very small compared to the best mid-latitude sites (see, e.g., Smith & Harper 1998). We will assume the following mean parameters derived considering summertime clear weather conditions: an ambient temperature 230°K, 0.09 emissive telescope, and emissivity of the lower atmosphere derived taking one minus the atmospheric transmission. The resulting background flux is shown in figure 2. A typical background flux with a bandpass filter ($\Delta\lambda \sim 1\mu\text{m}$) in the N band is about $10^8 e^-/\text{s}/\text{px}$. The full well of the detector is $2 \times 10^7 e^-/\text{px}$. Therefore we can adopt 10 Hz as the typical frame rate.

The detector quantum efficiency is very high, with a nominal value of 72% at T=10°K (see figure 3). Applying a constant bias voltage, we assume that the efficiency decreases by a factor 1.5 when the temperature is decreased from 10 to 5 °K. This effect can be countered by increasing the detector bias at the lower temperatures (see, e.g., Galdemard et al. 2002), so we will consider a constant value $\eta G \simeq 0.7$.

The array responsivity is quite uniform, with a standard deviation / mean ratio of 3.7%.

The array output transfer curve is found to be linear in slightly more than 90% of the dynamic range.

The dark current is not critical, but very high as many arrays designed for high flux applications. The expected dark current is $\sim 10^8 e^-/\text{s}/\text{px}$ at 10°K, and it is reduced at $\sim 10^5 e^-/\text{s}/\text{px}$ at 4°K. For comparison, the background radiation generates about $10^8 e^-/\text{s}/\text{px}$, and the back-

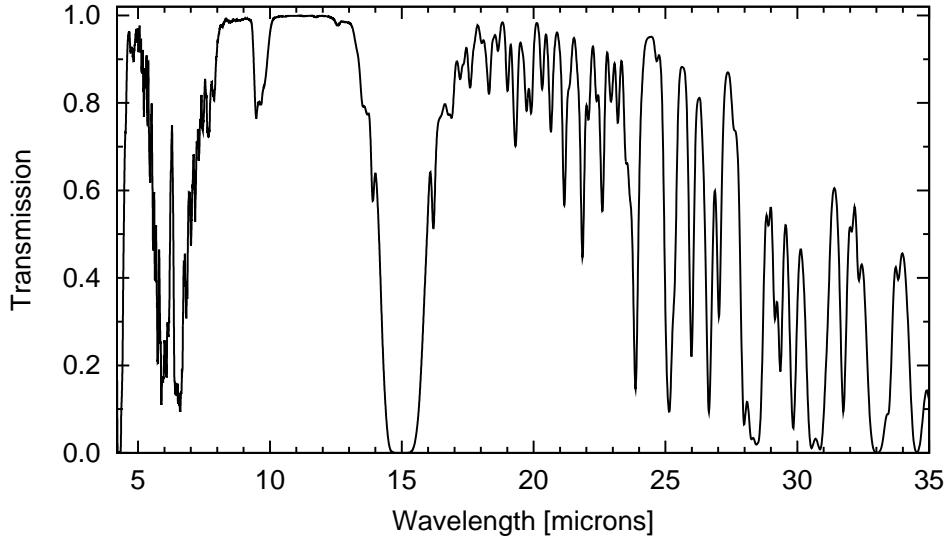


Fig. 1. Assumed atmospheric transmission at Dome C, derived from the considerations of Chamberlain et al. (2000).

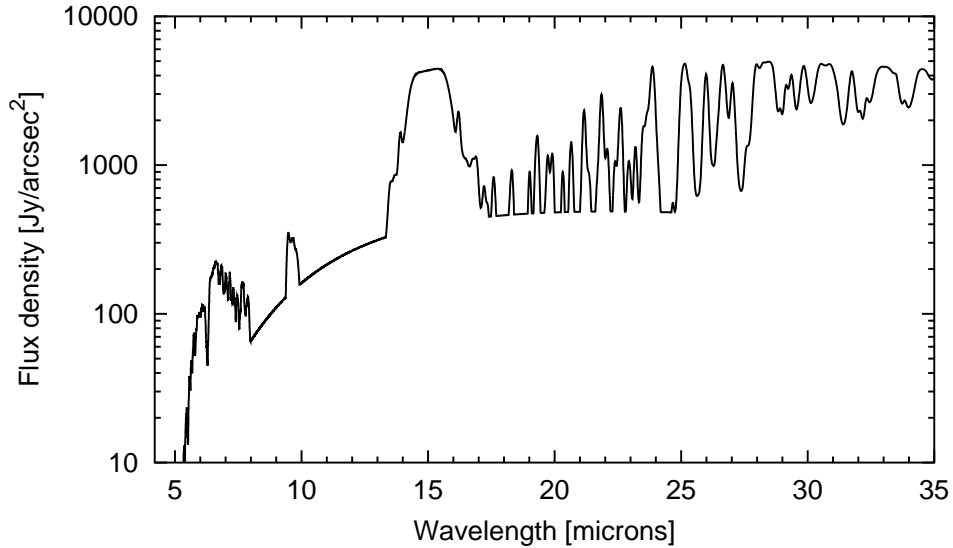


Fig. 2. Assumed background emission flux, obtained considering the telescope emissivity and the contribution of the thermal emission from the lower atmosphere, with $T=230^{\circ}\text{K}$.

ground limited performance (BLIP) is reasonably achieved for the working temperature of $6 - 7^{\circ}\text{K}$, where the dark current is $\sim 10^6 e^-/s/px$.

The readout noise is estimated around $600 e^-/px$. The BLIP condition is satisfied if each individual exposure time $t > t_{BLIP} \simeq 4\text{ms}$.

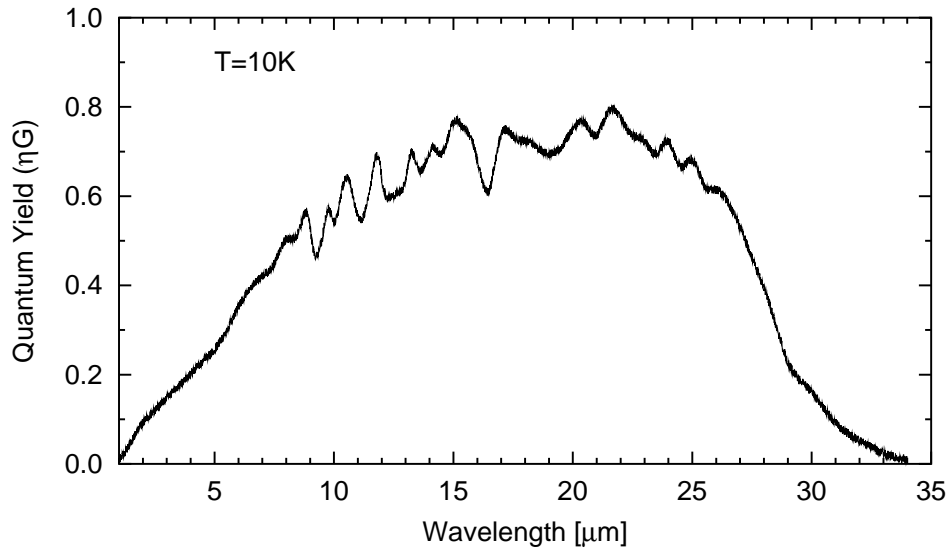


Fig. 3. Quantum yield of the Si:As BIB detector

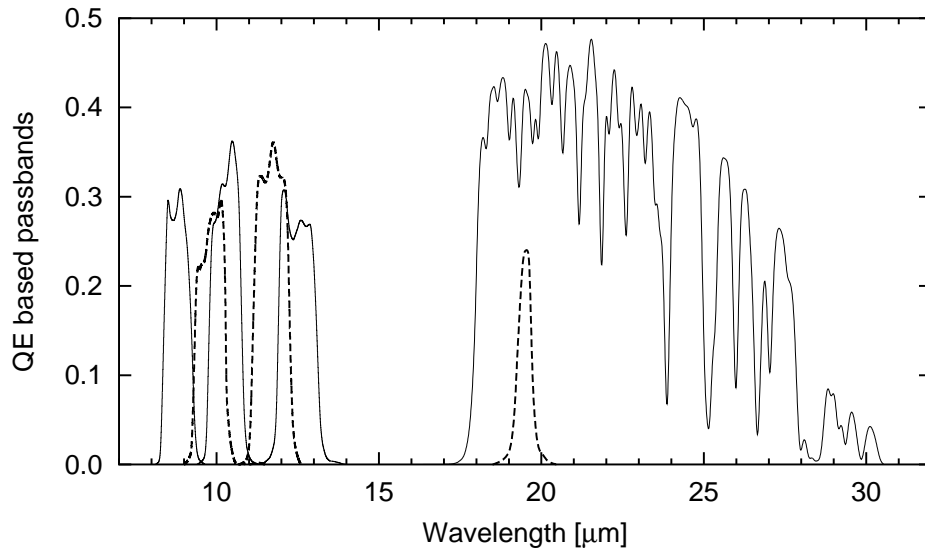


Fig. 4. Quantum efficiency based passbands: $(\eta G) \cdot (\tau_{atm} \tau_{tel} \tau_{det})$

2.1. Filter characterization

The preliminary filter system is made of 5 filters in the N window, 10% bandwidth, centered around 8.8, 9.8, 10.3, 11.7 and 12.5 μm . A bandpass filter centered around

19.5 μm , and a broad high-pass filter will be placed in the 18-30 μm range to exploit this atmospheric window accessible on the Antarctic Plateau. Figure 4 shows the passbands derived considering the array quantum efficiency (ηG), the atmospheric,

Table 2. Parameters of the photometric bands (in μm):

8.8	$\lambda_c = 8.81$	$K2$	$M2$	$1500K$	$800K$	$400K$	$200K$
	WHM = 0.87	$\lambda_{eff} = 8.78$	8.78	8.79	8.79	8.81	8.84
	$\lambda_o = 8.81$ $W_o = 0.82$	$W_{eff} = 0.81$	0.81	0.81	0.81	0.82	0.81
		$\lambda_{eff}(T) = 8.78 + 0.10 \Psi + 0.07 \Psi^2 - 0.04 \Psi^3$					
		$W_{eff}(T) = 0.81 + 0.04 \Psi - 0.09 \Psi^2 - 0.00 \Psi^3$					
9.8	$\lambda_c = 9.80$	$K2$	$M2$	$1500K$	$800K$	$400K$	$200K$
	WHM = 0.95	$\lambda_{eff} = 9.77$	9.77	9.77	9.78	9.79	9.83
	$\lambda_o = 9.81$ $W_o = 0.93$	$W_{eff} = 0.92$	0.92	0.93	0.93	0.93	0.92
		$\lambda_{eff}(T) = 9.77 + 0.09 \Psi + 0.07 \Psi^2 - 0.04 \Psi^3$					
		$W_{eff}(T) = 0.92 + 0.04 \Psi - 0.07 \Psi^2 - 0.01 \Psi^3$					
10.3	$\lambda_c = 10.27$	$K2$	$M2$	$1500K$	$800K$	$400K$	$200K$
	WHM = 1.01	$\lambda_{eff} = 10.24$	10.24	10.24	10.25	10.26	10.29
	$\lambda_o = 10.27$ $W_o = 0.98$	$W_{eff} = 0.97$	0.97	0.98	0.98	0.98	0.98
		$\lambda_{eff}(T) = 10.24 + 0.09 \Psi + 0.07 \Psi^2 - 0.04 \Psi^3$					
		$W_{eff}(T) = 0.98 + 0.04 \Psi - 0.07 \Psi^2 - 0.01 \Psi^3$					
11.7	$\lambda_c = 11.69$	$K2$	$M2$	$1500K$	$800K$	$400K$	$200K$
	WHM = 1.12	$\lambda_{eff} = 11.65$	11.65	11.65	11.66	11.67	11.70
	$\lambda_o = 11.69$ $W_o = 1.06$	$W_{eff} = 1.05$	1.05	1.06	1.06	1.06	1.06
		$\lambda_{eff}(T) = 11.65 + 0.08 \Psi + 0.08 \Psi^2 - 0.04 \Psi^3$					
		$W_{eff}(T) = 1.05 + 0.03 \Psi - 0.05 \Psi^2 - 0.01 \Psi^3$					
12.5	$\lambda_c = 12.50$	$K2$	$M2$	$1500K$	$800K$	$400K$	$200K$
	WHM = 1.16	$\lambda_{eff} = 12.45$	12.45	12.45	12.46	12.47	12.50
	$\lambda_o = 12.49$ $W_o = 1.09$	$W_{eff} = 1.08$	1.08	1.09	1.09	1.09	1.09
		$\lambda_{eff}(T) = 12.45 + 0.08 \Psi + 0.08 \Psi^2 - 0.04 \Psi^3$					
		$W_{eff}(T) = 1.09 + 0.03 \Psi - 0.04 \Psi^2 - 0.01 \Psi^3$					
19.5	$\lambda_c = 19.48$	$3000K$	$1500K$	$800K$	$400K$	$200K$	$100K$
	WHM = 0.49	$\lambda_{eff} = 19.47$	19.47	19.47	19.47	19.48	19.49
	$\lambda_o = 19.48$ $W_o = 0.55$	$W_{eff} = 0.55$	0.55	0.55	0.55	0.55	0.55
		$\lambda_{eff}(T) = 19.47 + 0.01 \Psi + 0.01 \Psi^2 - 0.00 \Psi^3$					
		$W_{eff}(T) = 0.55 + 0.00 \Psi - 0.00 \Psi^2 - 0.00 \Psi^3$					
22.5	$\lambda_c = 22.76$	$3000K$	$1500K$	$800K$	$400K$	$200K$	$100K$
	WHM = 9.48	$\lambda_{eff} = 21.15$	21.19	21.26	21.43	21.86	22.92
	$\lambda_o = 22.43$ $W_o = 6.91$	$W_{eff} = 6.36$	6.39	6.45	6.56	6.70	6.40
		$\lambda_{eff}(T) = 21.12 + 0.90 \Psi + 1.39 \Psi^2 - 0.49 \Psi^3$					
		$W_{eff}(T) = 6.33 + 1.02 \Psi - 0.14 \Psi^2 - 0.81 \Psi^3$					

telescope, and camera transmissions (τ). Table 2 reports the main parameters for each photometric bands: the central wavelength (λ_c), the width at half maximum (WHM), the effective wavelength (λ_o) and the effective width (W_o). Moreover, table 2 gives the effective wavelength and width obtained with simulated signals of late-type

stars and Planckian functions, and analytical formulae in function of $\Psi = 100^\circ K/T$ in the range from $T = 100^\circ K$ ($\Psi = 1$) to $T = 3000^\circ K$ ($\Psi \simeq 0$). These values can be useful for a fast evaluation of the photometric parameters for various astronomical sources.

Table 3. Sensitivity (for observations with chopping and nodding):

band	Camera + IRAIT		MIRAC3 + IRTF		COMICS + Subaru	
	S/N=1 t=3600s	S/N=10 t=900s	S/N=1 t=3600s	S/N=10 t=900s	S/N=1 t=3600s	S/N=10 t=900s
8.8	3 mJy	54 mJy	4 mJy	88 mJy	1 mJy	32 mJy
9.8	5 mJy	92 mJy	7 mJy	150 mJy	1 mJy	19 mJy
10.3	4 mJy	80 mJy	5 mJy	108 mJy	1 mJy	27 mJy
11.7	5 mJy	100 mJy	6 mJy	111 mJy	1 mJy	12 mJy
12.5	6 mJy	120 mJy	6 mJy	114 mJy	1 mJy	26 mJy
19.5	32 mJy	0.6 Jy			7* mJy	0.1* Jy
22.5	15 mJy	0.3 Jy	160* mJy	3* Jy	9* mJy	0.2* Jy

(*) the photometric bands are very different, and the value reported must be considered as a rough approximation

2.2. Sensitivity Estimates

We can evaluate the background limited performance (BLIP) using the following approximate formula:

$$S/N = 3.9 \times 10^3 \left[\frac{A \tau \eta G \Delta\lambda/\lambda t}{2 B_\nu \Omega_{source}} \right]^{1/2} f_\nu$$

where A is the telescope collecting area (m^2), τ is the overall transmission of camera, telescope, and atmosphere, η is the responsive quantum efficiency, G is photoconductive gain, $\Delta\lambda/\lambda$ is the fractional spectral bandwidth, B_ν is the background surface brightness (Jy/sr), Ω_{source} is the solid angle of the source (sr), t is the total integration time (s) for observations with chopping and nodding, and f_ν is the source flux density (Jy).

Table 3 shows the computed sensitivities for two cases: S/N=1 and a total integration time of 1 hour, S/N=10 and a total integration time of 15 minutes. The last columns show a comparison with two similar photometric systems: MIRAC3 mounted on the IRTF 3m Telescope (see, e.g., Hoffmann et al. 1998), and COMICS for the 8.2m Subaru Telescope (Okamoto et al. 2002). The first impression is that a 0.8m telescope at Dome C is equivalent to

a 3m telescope in a temperate site, and the exceptional performance in the Q band thanks to the expected exceptional atmospheric conditions, as Figs. 1 and 2 clearly show. One of the main targets of the IRAIT projects will be to verify these results that, if confirmed, will open a new era for mid-IR astronomy from ground.

References

- Chamberlain M. A., Ashley M. C. B., Burton M. G., et al., 2000, *ApJ* 535, 501
 Corcione L., Busso M., Porcu F., et al., 2003, *MSAIt* 74, 57
 Galdemard P., Garnier F., Mulet P., et al., 2002, in *Proc. SPIE* 4841, 129
 Hidas M. G., Burton M. G., Chamberlain M. A., et al., 2000, *PASA* 17, 260
 Hoffmann W. F., Hora J. L., Fazio G., et al., 1998, in *Proc. SPIE* 3354, 647
 Okamoto Y. K., Kataza H., Yamashita T., et al., 2002, *Proc. SPIE* 4841, 169
 Persi P., Ferrari-Toniolo M., Marenzi A. R., et al., 1994, *Exp. Astron.* 5, 365
 Persi P., Busso M., Corcione L., et al., 2002, in *Solids and Molecules in Space*, SIF Conf. Proc. 77, 205
 Smith C. H., Harper D. A., 1998, *PASP* 110, 747
 Tosti G., 2003, these Proceedings